Chemistry & Biology
Article

Semisynthetic Murine Prion Protein Equipped with a GPI Anchor Mimic Incorporates into Cellular Membranes

Diana Olschewski,[1] Ralf Seidel,[1] Margit Miesbauer,[2] Angelika S. Rambold,[2] Dieter Oesterhelt,[3] Konstanze F. Winklhofer,[2] Jörg Tatzelt,[2] Martin Engelhard,[1] and Christian F.W. Becker[1,*]
[1]Max-Planck Institute of Molecular Physiology, Department of Physical Biochemistry, Otto-Hahn-Str. 11, 44227 Dortmund, Germany
[2]Ludwig-Maximilians University Munich, Adolf-Butenandt-Institute, Schillerstrasse 44, 80336 Munich, Germany
[3]Max-Planck Institute of Biochemistry, Department of Membrane Biochemistry, Am Klopferspitz 18, 82152 Martinsried, Germany
*Correspondence: christian.becker@mpi-dortmund.mpg.de
DOI 10.1016/j.chembiol.2007.08.007

SUMMARY

Conversion of cellular prion protein (PrP^C) into the pathological conformer (PrP^{Sc}) has been studied extensively by using recombinantly expressed PrP (rPrP). However, due to inherent difficulties of expressing and purifying post-translationally modified rPrP variants, only a limited amount of data is available for membrane-associated PrP and its behavior in vitro and in vivo. Here, we present an alternative route to access lipidated mouse rPrP ($rPrP^{Palm}$) via two semisynthetic strategies. These rPrP variants studied by a variety of in vitro methods exhibited a high affinity for liposomes and a lower tendency for aggregation than rPrP. In vivo studies demonstrated that double-lipidated rPrP is efficiently taken up into the membranes of mouse neuronal and human epithelial kidney cells. These latter results enable experiments on the cellular level to elucidate the mechanism and site of PrP-PrP^{Sc} conversion.

INTRODUCTION

Transmissible spongiform encephalopathies (TSEs) are infectious neurodegenerative disorders that are characterized by conversion of cellular prion protein (PrP^C) into its pathological isoform, PrP^{Sc} [1–5]. These diseases affect humans and other mammalian species such as cattle (bovine spongiform encephalopathy), sheep, and goat (scrapie). Both isoforms of PrP exhibit significant differences in their biophysical properties, although their primary structure is identical [6–9]. Common features are a disulfide bond between α helices 2 and 3 [10] as well as the occurrence of a mixture of non-, mono-, and diglycosylated PrP variants and a C-terminal glycosylphosphatidylinositol (GPI) anchor [11, 12].

This latter feature is highly important for targeting PrP to membranes, and the GPI anchor seems to be important in the generation of PrP^{Sc} [13–15]; PrP linked to the plasma membrane via a heterologous CD4 transmembrane domain (PrP-CD4) is complex glycosylated as well [16–18]. However, in a scrapie-infected mouse neuroblastoma cell line, PrP-CD4 could not be converted into PrP^{Sc} [16, 17]. Several studies have provided substantial evidence that the key step in prion pathogenesis, the conversion of PrP^C into PrP^{Sc}, occurs on the outer leaflet of the cell membrane, with PrP anchored to the membrane via a C-terminal GPI anchor [19]. Additionally, in vitro experiments with raft preparations from PrP-infected and noninfected cells point to the fact that colocalization of PrP^C and PrP^{Sc} is a prerequisite for conversion of PrP^C into PrP^{Sc} [20–23].

Even though this seems to be direct evidence for the influence of membrane attachment of PrP on the process of conversion, many previous studies have only been performed with recombinantly produced, soluble PrP lacking any membrane anchor [24–27]. To the best of our knowledge, only three studies exist in which recombinantly expressed PrP harboring GPI anchor mimics was used to study membrane-anchored PrP^C and its transition into PrP^{Sc} without the need for isolation of PrP from detergent-resistant membranes [22, 23, 28]. In two of these studies, GPI mimics have been introduced at the C terminus of PrP via disulfide formation with specifically modified phospho- or sulfo-lipids, respectively, whereas the third study relies on a myristoyl moiety attached via a thioether bond. Here, we present two strategies for the semisynthesis of C-terminally modified PrP with chemically synthesized membrane anchor peptides based on the expressed protein ligation (EPL) approach [29] (Figure 1). One strategy relies on the expression of rPrP in fusion with the GyrA mini-intein and two affinity tags (His tag and chitin-binding domain), which allow for straightforward purification of the fusion construct from cell lysates. In order to generate rPrP with a C-terminal thioester moiety for native chemical ligation reactions with synthetic GPI anchor mimics, cleavage of the fusion protein was induced with an excess of alkyl thiols [30]. Subsequent addition of synthetic GPI anchor-mimicking peptides with N-terminal cysteine residues leads to chemoselective ligation of both reactants (Figure 1A). The second strategy avoids the generation and separation of a rPrP thioester

 ©2007 Elsevier Ltd All rights reserved

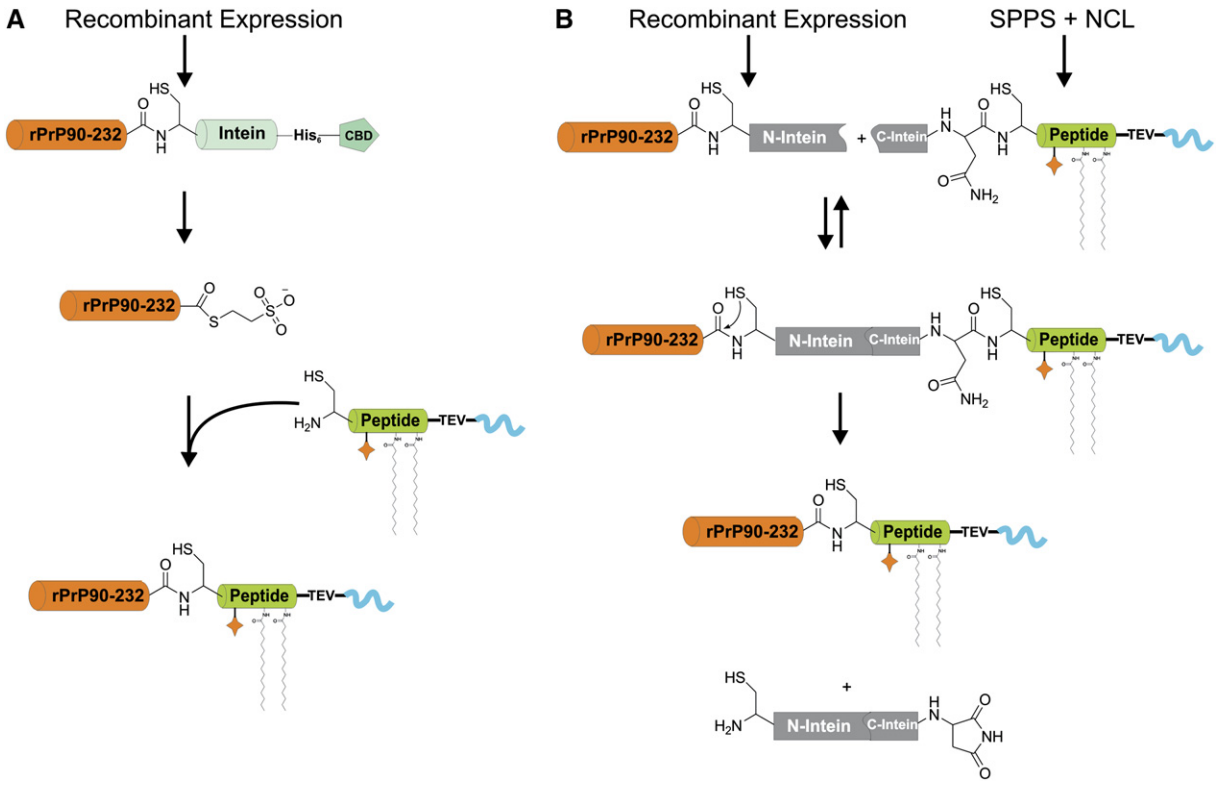

Figure 1. Strategies for the Semisynthesis of rPrP^{Palm}

(A) Generation of rPrP MESNA thioester from a rPrP-GyrA intein fusion construct expressed in *E. coli*.

(B) *Trans*-splicing reaction of a fusion construct of rPrP and the N-terminal part of the DnaE split intein (DnaE^{N}) expressed in *E. coli* with chemically synthesized GPI anchor mimic and the C-terminal part of the DnaE split intein (DnaE^{C}). Both strategies lead to the desired rPrP carrying a C-terminal GPI anchor mimic (rPrP^{Palm}).

species and is based on protein *trans*-splicing by expressing rPrP in fusion with the N-terminal segment of the DnaE split intein (DnaE^{N}) and synthesis of its C-terminal segment (DnaE^{C}) linked to GPI anchor-mimicking peptides [31, 32]. Both DnaE segments spontaneously associate when correctly folded and form a functional intein, which undergoes a series of *trans*-esterification steps in order to give the desired modified rPrP (Figure 1B). The advantage of our approach lies in the variety of the peptides, which can be tailor-made and can include not only alkyl chains in order to achieve membrane insertion, but also fluorescent labels for localization studies in vitro and in vivo as well as the introduction of cleavage sites for highly selective proteases. The latter feature provides a tool for controlled release of rPrP anchored in membranes. In vivo experiments reveal an insertion of the lipidated rPrP into the plasma membrane of mouse neuronal and human epithelial kidney cells.

RESULTS

Synthesis of GPI Anchor Mimics

Our goal was to produce lipidated peptides as GPI anchor mimics that would on the one hand target semisynthetic PrP proteins to membranes and, preferably, to liquid ordered (cholesterol- and glycosphingolipid-rich) domains. On the other hand, a site-specifically introduced fluorescent label should allow for in vitro and in vivo tracking of semisynthetic PrP equipped with GPI anchor analogs. These goals were achieved by testing a variety of different peptide sequences with one or two palmitoyl modifications that lead to a high affinity for liposomes as well as cell membranes [33]. Peptide synthesis was carried out by using the Fmoc-protection strategy, and incorporation of modifications such as fluorescent dyes and alkyl chains was achieved by applying orthogonal and pseudo orthogonal side chain-protection schemes. However, introducing two hexadecane chains into these membrane anchor peptides decreased their solubility in detergent and organic, solvent-free aqueous buffer systems dramatically and thereby prevented efficient ligation reactions with rPrP thioesters. In order to overcome these solubility problems, a short, oligoethylene glycol-like solubilization tag was introduced at the C terminus of the peptide, leading to a large increase in solubility (Figure 2A) [34, 35]. Using this strategy, ligation reactions could be carried out in the absence of detergent and organic solvent, and yields could be increased 4-fold. In Figure 2B, all peptides used as GPI anchor mimics are depicted; all of these peptides carry an N-terminal cysteine residue required for

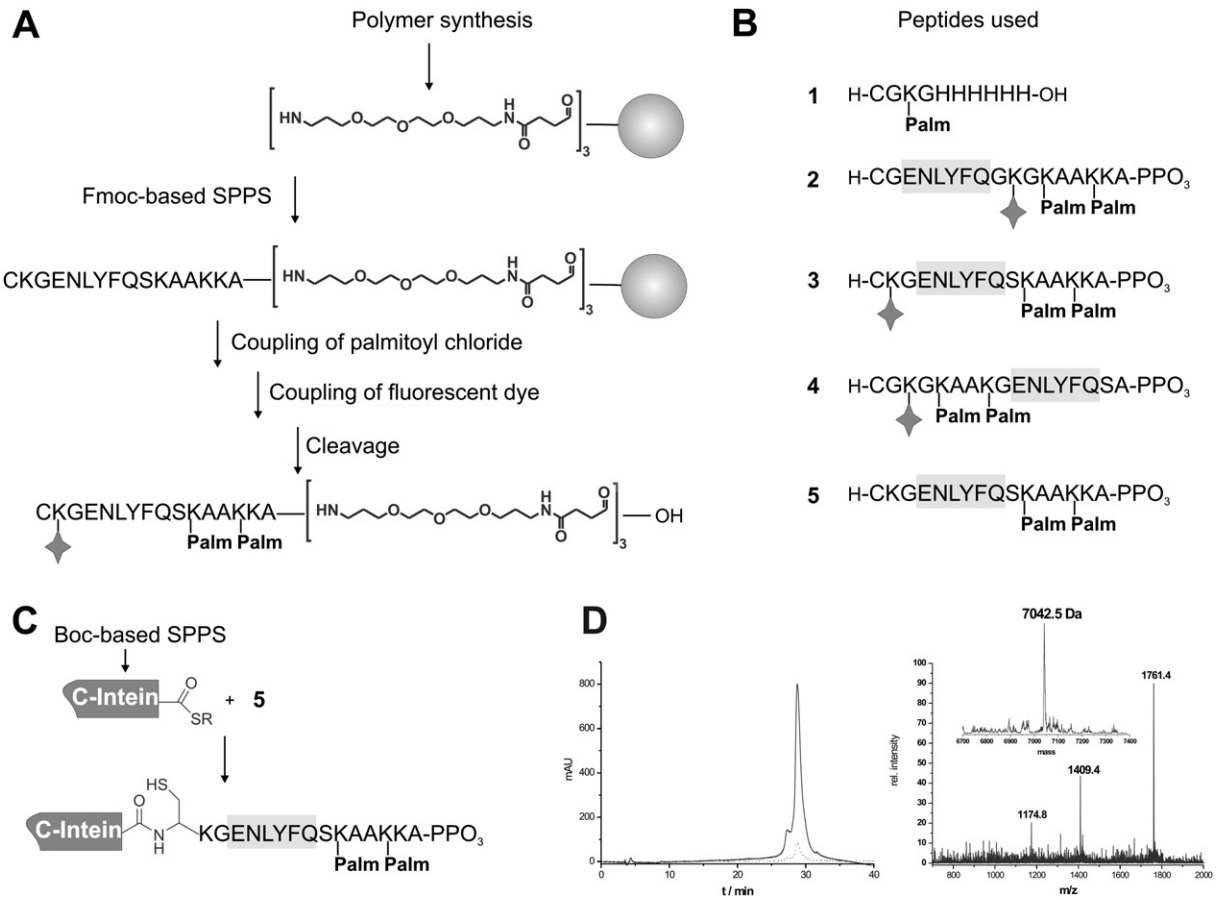

Figure 2. GPI Anchor-Mimicking Peptides

(A) Synthesis scheme of GPI anchor mimics. After coupling of three polyethyleneglycol polyamide building blocks as solubilization tags, a short peptide is assembled by Fmoc-based solid-phase peptide synthesis. Precleavage modification includes the coupling of two palmitoyl groups as membrane anchors and, in certain cases, the coupling of a fluorophore.

(B) Peptides used as GPI anchor mimics. In cases in which fluorescent labels are indicated, variants with and without such labels have been prepared.

(C) Native chemical ligation between DnaE^{C}-thioester and GPI anchor mimic peptide **3** to produce one of the DnaE^{C}-GPI anchor fusion peptides for *trans*-splicing reactions.

(D) RP-HPLC chromatogram of the DnaE^{C}-GPI anchor fusion construct after purification (left) and the corresponding ESI-mass spectrum of this compound (theoretical mass: 7051.8 Da; right).

native chemical ligation. Whereas peptide **1** contains only one palmitoyl group, peptides **2**–**5** share similar design features, including a tobacco etch virus (TEV) protease recognition site (ENLYFQ), two ivDde-protected lysine residues for attaching two palmitoyl chains, and one lysine residue protected with Mmt as a potential fluorescence-labeling site. Additionally, C-terminal polyethyleneglycol polyamide oligomer (PPO) modification is introduced to facilitate the handling and solubilization of peptides **2**–**5**. The functional groups are separated by spacer amino acids. Peptide **2** enables the cleavage of fluorescent label and palmitoyl groups from rPrP by proteolysis, whereas, with peptide **3**, the same cleavage reaction keeps the fluorescent label on rPrP. Peptide **4** allows for the removal of the solubilization tag (PPO_3), and peptide **5** resembles peptide **2**, except that the fluorescent label is omitted.

Synthesis and RP-HPLC purification of these GPI anchor mimics produced pure compounds that were obtained with yields ranging from 15% to 40% based on the amount of crude peptides. GPI anchor mimics **2**–**5** strongly associate with lipid bilayers, as was demonstrated by cell membrane binding studies. The corresponding nonpalmitoylated peptides did not associate with cell membranes at all (Figure S1, see the Supplemental Data available with this article online).

In order to use the GPI anchor-mimicking peptides for our *trans*-splicing strategy, the C-terminal domain of the DnaE split intein (DnaE^{C}) had to be connected with the N terminus of these peptides. This linkage was established by ligating the DnaE^{C}-peptide thioester (synthesized by Boc-solid-phase peptide synthesis [SPPS]) to the GPI anchor mimic peptides **2**–**5**. Figure 2C illustrates this reaction with GPI anchor mimic **5**. The ligation reaction was tested under a variety of conditions. A buffer system containing 6 M guanidine hydrochloride (GdnHCl) and 300 mM NaPi at pH 7.5 with thiophenol as ligation mediator

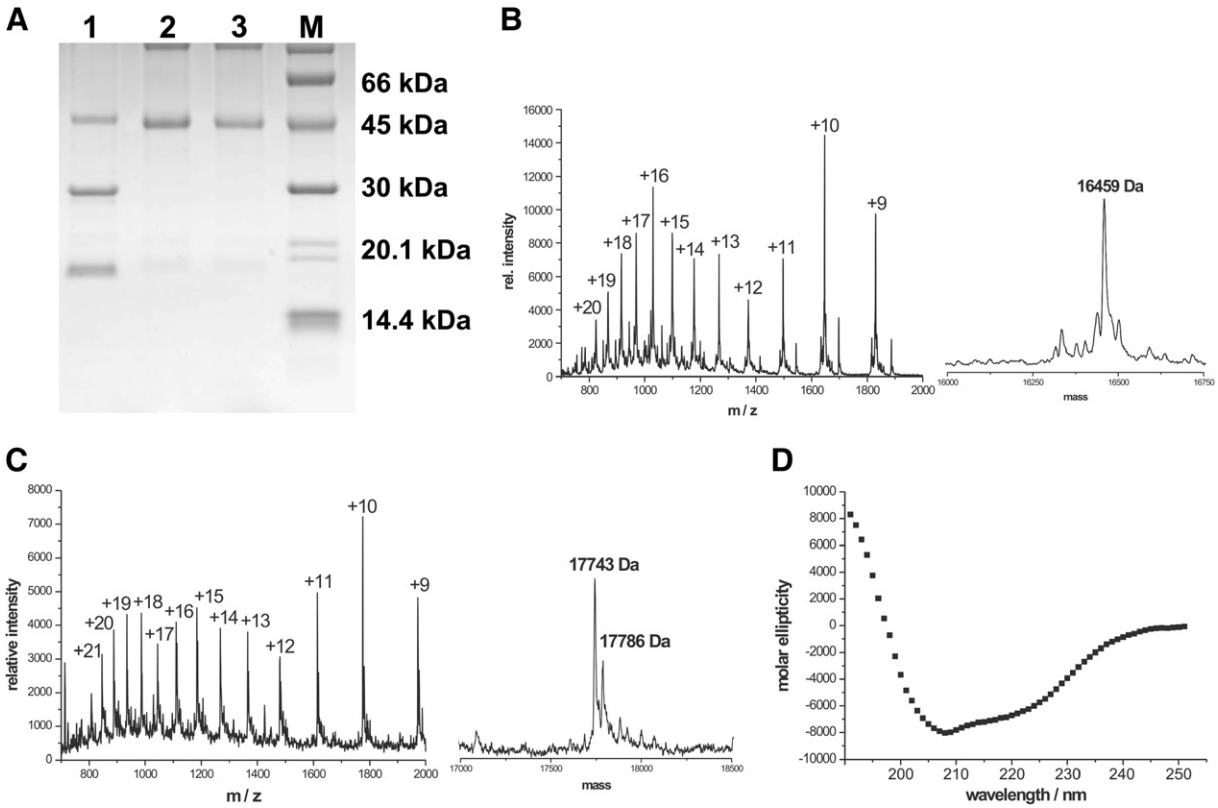

Figure 3. Expressed Protein Ligation to Generate rPrP^{Palm}

(A) SDS-PAGE of the rPrP-GyrA intein fusion protein after expression (lane 2, 8 μl; lane 3, 4 μl) and after inducing the cleavage reaction in 4 M urea buffer (pH 8.0) by adding 250 mM Mesna for 20 hr (lane 1). The band with an apparent molecular weight of 16 kDa corresponds to rPrP thioester, whereas the band at 30 kDa represents the GyrA intein.

(B) ESI-MS analysis of purified rPrP Mesna thioester (theoretical mass: 16,459.2 Da).

(C) ESI-MS of rPrP^{Palm} carrying the GPI anchor mimic **1** with only one palmitoyl group and a C-terminal His_6 tag (theoretical mass: 17,741.9 Da).

(D) CD spectrum of refolded rPrP^{Palm} (with GPI anchor mimic **1**) in 20 mM NaOAc (pH 5.0).

gave the best results, with yields of ~60%. The addition of detergent did not increase reaction yields when peptides containing a solubilization tag were used. By contrast, initial ligation experiments performed with peptides not equipped with a solubilization tag required the addition of detergents such as dodecylmaltoside (DDM) in order to obtain any ligation product. Adding lipids such as dodecylphosphocholine (DPC) to the ligation mixture had a beneficial effect on the ligation yield (an increase of up to 80% was observed in the case of peptide **4**). However, removal of DPC turned out to be highly problematic; therefore, ligations were carried out in the absence of any detergents or lipids. The purified fusion peptides consisting of the DnaE^{C} domain and the GPI anchor mimics **2**–**5** were obtained in reasonable purity and with yields between 18% and 30% (Figure 2D). The identity of the ligation products was confirmed by electrospray mass spectrometry, as shown for DnaE^{C}-**5** in Figure 2D.

Expression of PrP-Intein Fusion Proteins and Ligation Reactions

Murine PrP90-232 (rPrP) was expressed in *E. coli* as a fusion construct with the GyrA mini-intein from *Mycobacterium xenopi*. For this purpose, rPrP(90–232) was cloned into a modified pTXB3-vector (New England Biolabs) containing, in this order, the GyrA intein, a hexahistidine tag, and a chitin-binding domain (CBD) (Figure 1A). The fusion protein was expressed in inclusion bodies that could be solubilized in buffers containing 8 M urea or 8 M GdnHCl. Purification was achieved by Ni-NTA-based affinity chromatography. Productive cleavage of this fusion construct was observed after reducing the urea concentration down to 4 M in the presence of 250 mM mercaptoethanesulfonate (Mesna) (Figure 3A) [36]. No cleavage was observed in GdnHCl-containing buffers, even at concentrations of 2 M, at which the rPrP-GyrA fusion protein was still soluble. The resulting rPrP thioester was purified by RP-HPLC (isolated yield ~25%) and was used for native chemical ligation reactions with GPI anchor mimics **1**–**5**. A typical electrospray mass spectrum of purified rPrP thioester is shown Figure 3B.

Lipidated rPrP^{Palm} constructs were obtained with yields of ~30% when ligation reactions were carried out in 8 M urea buffers containing 17 mg/ml DPC as detergent (see Experimental Procedures). Figure 3C depicts an electrospray mass spectrum of the ligation product of rPrP

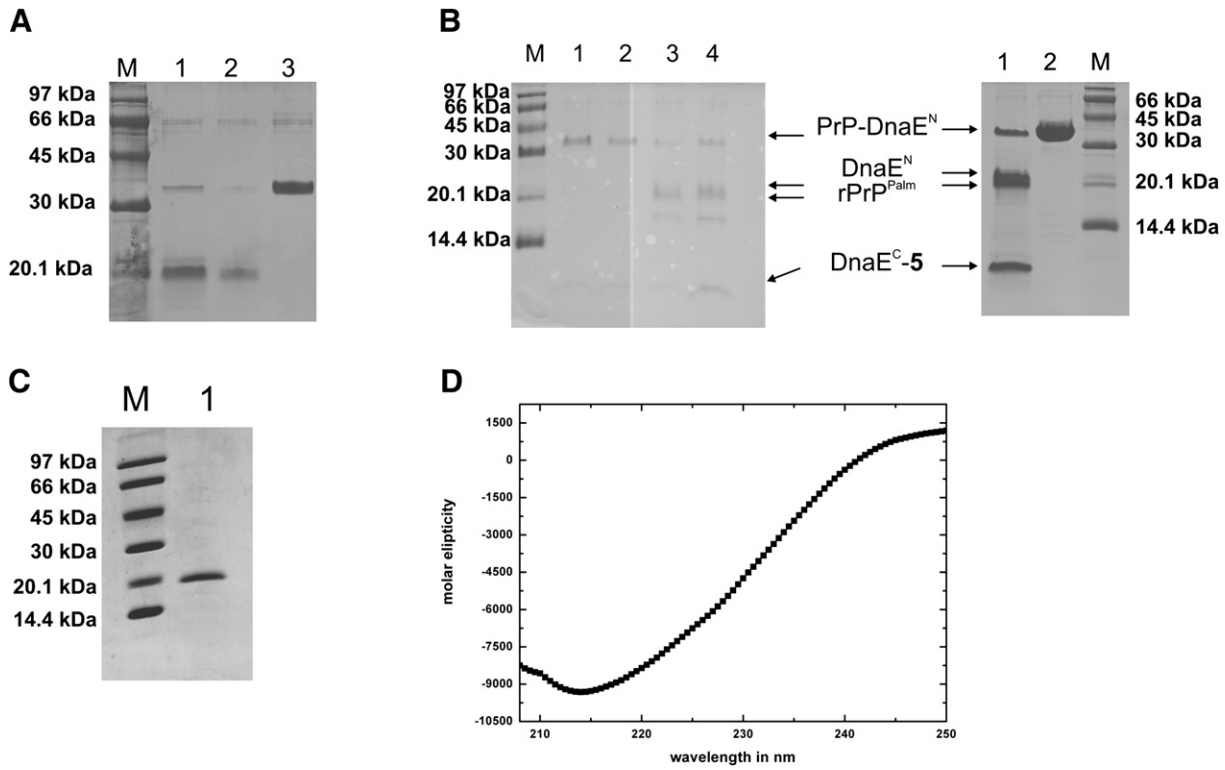

Figure 4. Protein *Trans*-Splicing to Generate rPrP^{Palm}

(A) SDS-PAGE of Ni-NTA purification of rPrP-DnaE^N fusion protein. Lane 1, flowthrough; lane 2, wash step; lane 3, elution from Ni-NTA.

(B) SDS-PAGE of rPrP-DnaE^N *trans*-splicing with DnaE^C-GPI anchor mimic **5** in 4 M urea-containing buffer (left gel, lane 3, 4 μl; lane 4, 8 μl) or chaotrope-free buffer (right gel, lane 1) and the purified rPrP-DnaE^N fusion construct (left gel, lane 1, 8 μl; lane 2, 4 μl; right gel, lane 2).

(C) SDS-PAGE of purified rPrP^{Palm} (with nonfluorescent GPI anchor mimic **5**) in lane 1.

(D) CD spectrum of rPrP^{Palm} in DOPC liposomes in 150 mM NaCl, 50 mM Tris-HCl (pH 8).

thioester and GPI anchor peptide **1**. Two mass peaks can be identified in the deconvoluted spectrum, one that corresponds to the theoretical mass of 17,743 Da, and a second one with a mass of 17,786 Da. This mass increase of 43 Da is most likely caused by carbamylation of rPrP^{Palm}, at a primary amino group, a typical side reaction when handling proteins for extended periods of time in urea-containing buffers. The site of modification was not further investigated. After refolding in 20 mM NaOAc buffer at pH 5, CD spectroscopic measurements revealed a predominantly α-helical structure of this rPrP^{Palm} variant, corresponding to the cellular form of PrP (Figure 3D). Reconstitution into 1,2-dioleoyl-*sn*-glycero-3-phosphocholine (DOPC) liposomes and subsequent ultracentrifugation proved that almost 50% of the single-palmitoylated rPrP^{Palm} remained in the supernatant and did not efficiently attach to the liposomes (data not shown), in accordance to previous investigations on lipidated Ras [37].

In order to produce lipidated rPrP^{Palm} via a *trans*-splicing approach, a fusion construct of rPrP with the N-terminal part of the naturally occurring split intein DnaE from *Synechocystis* (DnaE^N) was cloned into the vector pTXB3. The rPrP-DnaE^N fusion construct was also expressed as insoluble aggregates in *E. coli* and required a solubilization step in 8 M GdnHCl, followed by Ni-NTA affinity purification (Figure 4A). Partial refolding of the fusion protein and generation of a functional split intein was achieved in two different ways. In a first attempt, the chaotrope concentration was reduced stepwise to 4 M urea by dialysis. At 4 M urea, *trans*-splicing was observed when adding DnaE^C peptide to the rPrP-DnaE^N fusion construct (Figure 4A). *Trans*-splicing was almost quantitative (~90%) under these conditions, but it was very slow. A second strategy proved more successful and led to almost quantitative folding of rPrP-DnaE^N by diluting the purified protein 10-fold into a glutathione- and L-arginine-containing buffer. Subsequent dialysis against a Tris-buffered solution (pH 7.5) gave active rPrP-DnaE^N fusion proteins that produced the *trans*-splicing product with similar yields (~90%, Figure 4B). Nevertheless, the chaotrope-free splicing reaction was ~4 times faster when compared to the reaction in 4 M urea (1 day compared to 4 days), and no carbamylation was observed when using the second strategy. Different detergents were also tested, and non-ionic ones such as octylglycoside (OG) and DDM gave the best results, with yields around ~50%–90% based on the splicing product rPrP^{Palm}. However, to achieve these high *trans*-splicing yields, it was necessary to add low concentrations (5–10 mM) of reducing agents such as MESNA, DTT, or TCEP. Similar *trans*-splicing reactions

were carried out with the DnaE^{C}-GPI anchor mimic fusion construct attached to DOPC vesicles and the subsequent addition of rPrP-DnaE^{N}, leading to similar yields to those described for detergent-containing buffers. Due to these advantages, all further experiments were carried out with lipidated rPrP produced by *trans*-splicing under chaotrope-free conditions with GPI anchor mimic **5**. rPrP variants with GPI anchor mimics **2**–**4** behaved similarly to rPrP^{Palm} equipped with **5** in folding and aggregation assays.

Purification and Folding of rPrP^{Palm}

Purification of rPrP^{Palm} was achieved by Ni-NTA affinity chromatography to remove unreacted rPrP-DnaE^{N} and DnaE^{N} and subsequent gel filtration. The purified material was analyzed by SDS-PAGE (Figure 4C). In order to obtain correctly folded rPrP^{Palm}, the purified protein was first unfolded in a buffer containing 6 M GdnHCl as well as glutathione and its oxidized form (GSSG). Subsequently, the solution was rapidly diluted into sodium acetate buffer (20 mM, pH 5) containing DOPC vesicles. This refolding procedure was initially tested with rPrP in the absence of lipid vesicles, and the resulting rPrP was checked by CD spectroscopy as well as NMR experiments, which verified folding into the predominantly α-helical cellular form (data not shown). For rPrP^{Palm}, CD spectroscopy was carried out in a similar buffer containing DOPC vesicles confirming the α-helical structure of rPrP^{Palm} after refolding (Figure 4D). These rPrP and rPrP^{Palm} preparations were stable at pH 5.0 for up to 48 hr at 4°C and could also be stored at −80°C for prolonged periods of time without any indication of aggregation. This folding procedure is based on results obtained for nonlipidated PrP samples [38]. No difference between the secondary structure of membrane-bound rPrP^{Palm} and rPrP was found in our experiments, which is consistent with data reported previously for membrane-associated variants of PrP [21–23].

Aggregation into a proteinase K (PK)-resistant rPrP variant (rPrP^{res}) can be induced by adding chaotrope mixtures such as 3 M urea/1 M GdnHCl at slightly acidic pH. Formation of rPrP^{res} is observed in GdnHCl/urea-containing buffers after 15 hr for rPrP in the presence and absence of liposomes and also after 15 hr for rPrP^{Palm} in the absence of liposomes. Significantly, under similar conditions (same concentration at 37°C), the formation of PK-resistant rPrP^{Palm} is much slower in the presence of liposomes. Resistant material is not observed after 15 hr, but only after 36 hr (Figure 5A). These results indicate that membrane anchoring of rPrP^{Palm} reduces the speed of aggregate formation, thereby slowing down the conversion into rPrP^{res}. Accordingly, results were obtained by using thioflavin T fluorescence assays that indicate a faster aggregation of rPrP in buffers with and without liposomes (aggregation starts after 1 hr at 37°C) when compared to rPrP^{Palm} in buffer with liposomes (aggregation starts after 15 hr at 37°C) (Figure 5B). Such a faster aggregation was also observed for rPrP^{Palm} in the absence of DOPC liposomes (Figure 5B). Therefore, a direct influence of liposomes on aggregation rates of rPrP without a membrane anchor can be excluded.

Vesicle Association

Reconstitution of rPrP^{Palm} (rPrP + GPI anchor mimic **5** was used here) into liposomes was achieved by dilution of a detergent-containing solution of rPrP^{Palm} into a liposome-containing buffer and subsequent removal of DDM by treatment with biobeads. Membrane insertion of rPrP^{Palm} with two palmitoyl modifications is almost quantitative. Unambiguous proof that rPrP^{Palm} is attached to DOPC vesicles via its two C-terminal palmitoyl chains was provided by sucrose density gradient centrifugation. rPrP^{Palm}-containing fractions were obtained at densities of ~10%. Treating these vesicles for 6 hr with TEV protease removed rPrP from its lipid anchor, and it is therefore found in the top layer of the sucrose gradient (Figure 5C). These data clearly indicate that proteolytic removal of the palmitoyl anchor from rPrP^{Palm} leads to detachment of rPrP from the vesicles and proves that the rPrP^{Palm}-vesicle interaction is mediated by the alkyl chains of the palmitoyl groups. Therefore, unspecific hydrophobic interactions of rPrP with vesicle membranes can be ruled out.

Cellular Uptake

Strong interactions of the double-palmitoylated and fluorescently labeled peptides and proteins with cell and artificial membranes were already demonstrated (Supplemental Data) [33]. However, no evidence has so far been presented that rPrP^{Palm} modified with a GPI anchor mimic can be efficiently attached to cells via insertion into their membrane. In order to demonstrate that the GPI anchor mimic **5** confers the ability to insert into cell membranes to rPrP^{Palm}, we incubated murine neuronal cells (N2a) (Figure 6) and human embryonic kidney (HEK293T, data not shown) cells with 0.01 mg/ml rPrP^{Palm} suspended in a liposome preparation in phosphate-buffered saline (PBS). In control experiments, rPrP, devoid of the GPI anchor mimic, was used at similar concentrations (Figure 6). It should be noted that transfer efficiencies were highly dependent on the composition of the liposomes used for protein transfection assays. Initial experiments with rPrP^{Palm} reconstituted in DOPC liposomes as well as with rPrP^{Palm} in detergent micelles such as OG and DDM did not lead to any transfer of soluble rPrP^{Palm} into live cells. In the case of DOPC liposomes, no rPrP^{Palm} was detected in the cells—neither by western blot analysis of lysed cells, nor by immunofluorescence analysis of fixed cells. For rPrP^{Palm}, in detergent-containing buffers, western blot analysis indicated that a small amount of rPrP^{Palm} was associated with the cell debris after lysis; however, membrane extraction with Triton X-100 and sodium deoxycholate (DOC) did not produce any soluble rPrP^{Palm}. This result and the fact that viability of the cells could only be maintained for a period of 1 to a maximum of 4 hr in the presence of detergent made clear that a different strategy was required to efficiently transfer rPrP^{Palm}.

Cellular uptake was achieved by adding rPrP^{Palm} and rPrP(90–232) samples to the growth media at pH 7.3 after reconstitution into a liposome-forming transfection agent (Pro-Ject, Pierce) and incubation at 37°C in Petri dishes.

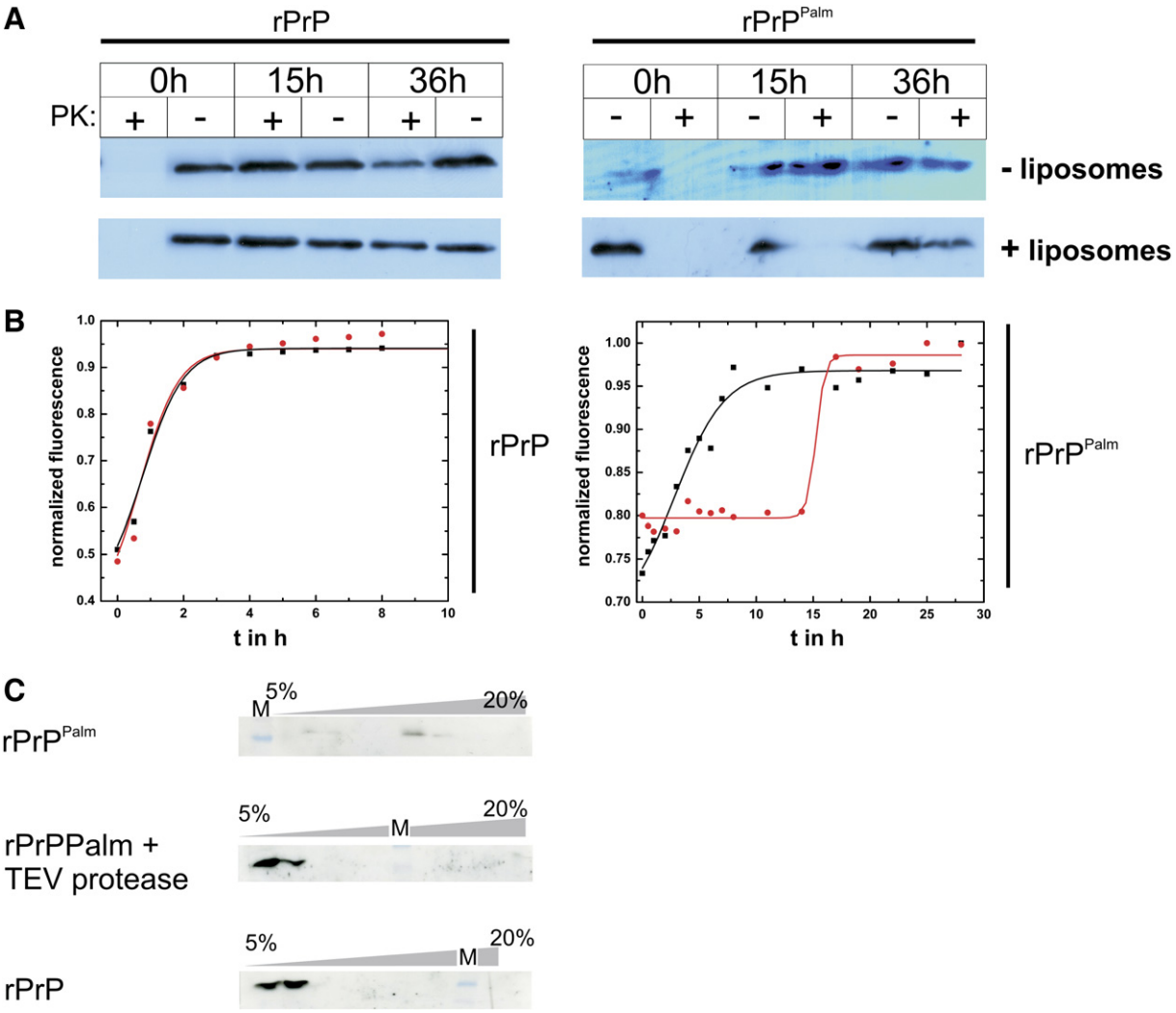

Figure 5. In Vitro Analysis of rPrP^{Palm}

(A) Proteinase K resistance of rPrP (left) and rPrP^{Palm} (right) after incubation in aggregation buffer (3 M urea, 1 M GdnHCl, 150 mM NaCl, 20 mM NaPi [pH 6.8]). Proteinase K-resistant rPrP is already observed after 15 hr of incubation at 37°C in the presence and absence of liposomes; however, PK-resistant rPrP^{Palm} only appears after 36 hr of incubation in the presence of liposomes.

(B) Thioflavin T (ThT) assay carried out at 37°C with aggregation buffer. An increase in ThT fluorescence at 488 nm indicates the presence of aggregated material. A steep increase in absorbance is observed for rPrP (left panel) after 30 min in the presence (red circles) and absence (black squares) of liposomes, whereas rPrP^{Palm} aggregation leads to an increase in ThT fluorescence after 15 hr in the presence of liposomes (right panel, red circles). In the absence of liposomes, rPrP^{Palm} aggregation starts after 1–2 hr (black squares).

(C) Sucrose gradient centrifugation of rPrP^{Palm}, rPrP^{Palm} treated with tobacco etch virus (TEV) protease for 6 hr at room temperature, and rPrP in DOPC liposomes. A capital "M" indicates the position of the prestained marker on the depicted western blots. rPrP^{Palm} associates with DOPC liposomes and can be found at concentrations of 10% sucrose. rPrP^{Palm} after treatment with TEV protease, which cleaves rPrP from its GPI anchor mimic C-terminal peptide, is found at the lowest sucrose concentration, similar to rPrP, which should not associate with liposomes.

After 2 and 5 hr, respectively, cells were washed, harvested, and lysed in a buffer containing 0.5% Triton X-100 and 0.5% DOC in PBS. This buffer is known to efficiently solubilize native PrP^{C} and should therefore also be able to extract rPrP^{Palm} if it is bound to the membrane in a nonaggregated state [39]. The cell lysate was fractionated by centrifugation, and PrP present in the detergent-soluble (Sup) and -insoluble fraction (Pellet) was detected by western blot with the monoclonal antibody 3F4. This antibody is specific for the externally added rPrPs and does not react with endogenous mouse PrP^{C} [40].

After addition to the cells, rPrP could only be recovered in a detergent-insoluble conformation (Figure 6A, pellet), indicating a rapid misfolding after dissolving rPrP in cell culture media. In contrast to this observation, up to 50% of the total rPrP^{Palm} was found in the supernatant after 5 hr of incubation. Obviously, rPrP^{Palm} maintains a correct conformation, most likely by integrating into the plasma

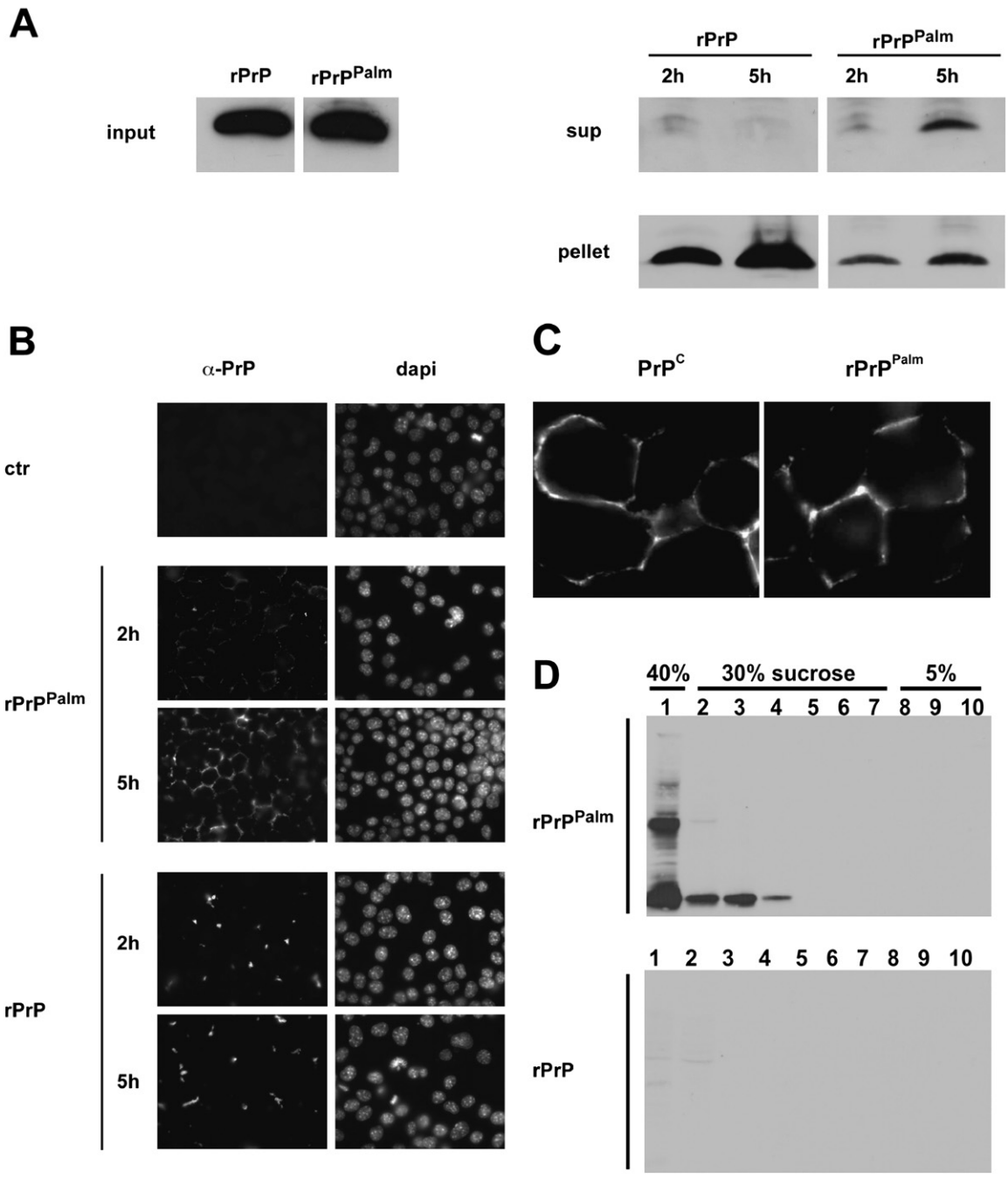

Figure 6. Cellular Uptake of rPrP^{Palm} into N2a Cells

N2a cells were transfected with rPrP^{Palm} and rPrP and incubated for 2 hr and 5 hr, respectively, at 37°C.

(A) Cells were harvested, lysed in cold buffer C, and fractionated by centrifugation. rPrP present in the detergent-soluble (sup) and -insoluble (pellet) fraction was analyzed by western blot with the mAb 3F4. As input controls, recombinant PrPs were incubated in the absence of cells, precipitated with TCA, and analyzed by western blot.

(B) For immunofluorescence studies, cells were grown on coverslips, incubated with rPrPs, fixed, and permeabilized. rPrP and rPrP^{Palm} were detected with the mAb 3F4. Nuclei were stained with DAPI.

(C) Higher-resolution images of N2a cells transfected with PrP^{C} and rPrP^{Palm}. mAb 3F4 was used to detect PrP^{C} and rPrP^{Palm}.

(D) Western blot analysis of rPrP and rPrP^{Palm} after extraction from cell membranes with cold Triton X-100 and a subsequent flotation assay in a sucrose gradient.

membrane via its GPI anchor mimic. Extraction of transfected N2a cells with cold Triton X-100-containing buffer, followed by a flotation assay on a sucrose gradient, was used to determine if $rPrP^{Palm}$ associates with detergent-insoluble membrane domains similarly to what is described for $rPrP^{C}$ [41, 42]. In this assay, rPrP remains in the pellet of the low-spin centrifugation and does not float in the sucrose gradient, whereas $rPrP^{Palm}$ floates in fractions 1–4 at concentrations of 30%–40% sucrose (Figure 6D). This result indicates a difference between PrP^{C} and $rPrP^{Palm}$ that is probably due to the chemical nature of the native GPI anchor and the GPI anchor mimic. In order to analyze the cellular localization of externally added rPrP and rPr^{Palm}, indirect immunofluorescence experiments were performed. In N2a cells incubated with $rPrP^{Palm}$ as described above and treated with the antibody 3F4, which is specific for $rPrP^{Palm}$, cell boundaries are clearly visible, revealing that the majority of $rPrP^{Palm}$ is located at the plasma membrane (Figure 6B). However, for rPrP, no staining of cell membranes was observed. In this case, only small, bright spots, which are probably due to large rPrP aggregates, occurred. Similar pictures were obtained by Breydo et al. with myristoylated rPrP [28]; but, in this work, no membrane extraction experiments, which could have distinguished between soluble and insoluble PrP associated with cell membranes, were described. DAPI staining confirmed that all cells were viable, and a negative control demonstrates that no endogenous PrP was picked up by this method (Figure 6). Higher-resolution images of N2a cells transfected with $rPrP^{Palm}$ and cellular Prp^{C} (in mammalian expression vector pcDNA3.1 [18]) clearly demonstrate that transient transfection with DNA coding for PrP^{C} carrying the 3F4 epitope and detection with the same antibody (3F4) leads to a similar cell surface-staining pattern as transfection with $rPrP^{Palm}$ (Figure 6C).

DISCUSSION

Previously reported approaches to obtain recombinantly expressed, membrane-bound PrP relied on the formation of disulfide bonds between either a PrP variant with a 6 amino acid C-terminal extension consisting of 5 glycine residues and a C-terminal cysteine with a thiol-reactive lipid (N-((2-pyridyldithio)-propinyl)-1,2-dihexadecanoyl-sn-glycero-3-phosphoethanolamine) already incorporated into liposomes, or a PrP variant containing a mutation of the C-terminal serine residue 231 to a cysteine that was reacted with 3-(hexadecane-1-sulfonyl)-2-(hexadecane-1-sulfonylmethyl) propionic acid linked to a methanethiosulfonate reactive group via a polyethylene glycol linker [22, 23]. Both approaches suffer from both the fact that a free thiol group has to be maintained at the C terminus of rPrP while an intact disulfide bridge must be conserved to ensure structural integrity of the protein during folding and subsequent measurements as well as from the sensitivity of the formed disulfide bond between rPrP and the respective membrane anchor to reducing conditions. A recently described myristoyl-modified PrP variant was produced by reacting N-(2-myristoylamidoethyl-)maleimide with PrP carrying a cysteine at position 230 [28].

The two semisynthetic strategies that are described here do not require the maintenance of such a delicate equilibrium between a free thiol group and an intact disulfide bond inside the recombinantly expressed PrP molecule; however, for one of them, a C-terminal thioester moiety is needed to perform a native chemical ligation reaction with a peptide containing an N-terminal cysteine residue, and this reaction requires the addition of nucleophilic thiols (and therefore reducing conditions) in order to accelerate the ligation reaction and suppress unwanted side reactions (Figure 1A) [30]. The second strategy, involving the split intein approach, does not require isolation of such a thioester species and strongly reducing conditions can be avoided, which allows the internal disulfide bond of folded rPrP to stay intact (Figure 1B). Furthermore, the absence of high concentrations of thiols would allow for the extension of this method toward in vivo applications [32]. In both cases, a stable amide bond results from these synthesis strategies and provides a distinct advantage over reduction-prone disulfide bonds, especially in in vivo applications.

In this study, both approaches led to recombinant α-helical PrP with a variety of C-terminal GPI anchor mimics ($rPrP^{Palm}$) in multimilligram amounts, with total yields of ~10% based on the expression of rPrP fusion proteins in *E. coli*. To our knowledge, the resulting $rPrP^{Palm}$ variants constitute a first example of applying EPL and *trans*-splicing toward proteins that are, due to their disposition to aggregate, inherently difficult to handle and that play an important role in conformational protein diseases. A series of denaturation and renaturation steps was required to obtain functional rPrP-intein fusion proteins as well as folded $rPrP^{Palm}$.

The system finally chosen to produce $rPrP^{Palm}$ with GPI anchor mimic **5** for aggregation and transfection assays consisted of rPrP-$DnaE^{N}$ fusion protein and the $DnaE^{C}$-GPI anchor mimic fusion peptide. *Trans*-splicing reactions were carried out in chaotrope-free, detergent-containing buffer with low concentrations of reducing reagents. The positive effect of these reducing reagents on *trans*-splicing yields can most likely be explained by keeping cysteine side chains that are involved in *trans*-esterification steps during *trans*-splicing in their active, reduced state (Figure 1B). The observation that *trans*-splicing occurs efficiently in buffers containing DOPC liposomes with one vesicle-anchored component points toward the feasibility of such *trans*-splicing reactions in membranes of live cells if the fully functional, reactive cysteine side chains can be retained.

We have tested the tendency of vesicle-attached $rPrP^{Palm}$ to aggregate by two different, well-established methods, one being proteinase K resistance and the other thioflavin T binding [43]. Both assays provide evidence that aggregation of vesicle-attached $rPrP^{Palm}$ proceeds slower (by a factor of 5–6) than aggregation of rPrP in control experiments at similar concentrations. We deduce from these experiments that membrane-attached $rPrP^{Palm}$

is less prone to refold into the β sheet-rich $rPrP^{res}$ variant due to stabilizing effects of the lipid bilayer. The effect of membrane association of PrP variants on their tendency to form proteinase K-resistant aggregates is still a matter of debate since it has been reported that no influence of membrane anchoring on PrP stability can be observed for lipidated rPrP [22]. However, data based on either rPrP equipped with a lipid anchor or PrP from mammalian cells carrying a GPI anchor suggest that membrane anchoring protects PrP from conversion into its proteinase K-resistant state [21, 23, 44]. These latter results are in agreement with the effect observed for $rPrP^{Palm}$ in which aggregation occurs much slower when exposed to conditions that trigger aggregation of rPrP. The influence of lipid composition and the charge of the lipid head groups as well as localization of $rPrP^{Palm}$ in ordered membrane domains on PrP conversion are still controversially discussed. This discussion might possibly be resolved by further cell-based studies with $rPrP^{Palm}$. It is important to note that no binding of rPrP to DOPC liposomes was observed, and that $rPrP^{Palm}$ was detached from such liposomes by treatment with TEV protease by taking advantage of the designed cleavage site in our GPI anchor mimic **5**. This indicates that the N-terminally truncated rPrP(90–232) variant used here does not insert into zwitterionic liposomes, in contrast to reports about rPrP in negatively and uncharged membranes [19, 44]. Furthermore, it can be concluded that $rPrP^{Palm}$ is solely attached to the outside of the vesicles, and that only a minor amount of $rPrP^{Palm}$, which is not detected by western blot, is found in the buffer, indicating its very strong binding to the lipid bilayer.

Having established the specific attachment of $rPrP^{Palm}$ to lipid bilayers, the incorporation into the plasma membrane of live cells was elucidated. This step is crucial for further investigating prion biochemistry. Anchoring of $rPrP^{Palm}$ into the cell membrane is inherently difficult since transfer of $rPrP^{Palm}$ from one membrane environment to the outer leaflet of the cell membrane has to occur, as it was demonstrated by the unsuccessful attempts with different lipids and detergents. Finally, a protein transfection agent (Pro-Ject, Pierce) that consists of cationic lipids turned out to be successful. An explanation for this behavior could be that a direct transfer from liposomes to the plasma membrane only rarely (if at all) occurs. However, if fusion is facilitated, in the present case due to electrostatic attraction between positively charged Pro-Ject liposomes and negatively charged cell membranes, an efficient delivery of $rPrP^{Palm}$ can occur. It is important to note that proof of correct incorporation of $rPrP^{Palm}$ into the plasma membrane cannot be provided by simple indirect immune fluorescence with an rPrP-specific antibody. This method does not allow for the distinction between aggregated $rPrP^{Palm}$ associated with cell surfaces and soluble $rPrP^{Palm}$ attached to the membrane via its GPI anchor mimic. Therefore, we included control experiments based on extraction of cell membranes with Triton X-100 and DOC-containing buffers. These experiments provided proof that a soluble variant of $rPrP^{Palm}$ is attached to the membrane, and western blot analysis of membrane extracts and pellets is crucial to gain information about the state of membrane-associated rPrP variants. A flotation assay revealed more evidence that $rPrP^{Palm}$ associates with the cell membrane. Although $rPrP^{Palm}$ was detected at different sucrose concentrations than PrP^{C}, this was to be expected because of the different chemical nature of the GPI anchor mimic.

The similar cell surface-staining patterns of N2a cells transfected with $rPrP^{Palm}$ and PrP^{C} provide additional proof for similar membrane insertion of semisynthetic $rPrP^{Palm}$ with a GPI anchor mimic and PrP^{C} with a native GPI anchor. The successful transfer of $rPrP^{Palm}$ into cell membranes of two different cell lines paves the way for future studies of the conversion process of membrane-anchored $rPrP^{Palm}$ in live cells either by western blot analysis of fractionated cell lysates or, with much higher resolution, by in vivo fluorescence analysis of fluorescently labeled $rPrP^{Palm}$ variants.

SIGNIFICANCE

Toxic conformations of cellular proteins are the cause for several severe neurodegenerative diseases for which no therapeutic regiment exists to date. The prion protein (PrP) is special among these proteins because it is an infectious agent that can convert correctly folded PrP into its toxic isoform. The elucidation of this process is of central importance for understanding the nature of toxic protein conformations and the mechanism of their generation. The cellular form of PrP itself is probably converted into its misfolded isoform in its natural environment, the outer leaflet of the cell membrane. In order to elucidate this process of conversion and the subsequent processing inside cells, we have established two semisynthesis strategies to obtain multimilligram amounts of C-terminally modified recombinant PrP. These strategies allow for the synthesis of correctly folded rPrP variants with GPI anchor mimics at their C termini ($rPrP^{Palm}$) that attach to liposomes via their GPI anchor mimics and thereby afford the possibility to study membrane-attached rPrP. Such liposome attachment slows the formation of proteinase K-resistant aggregates of $rPrP^{Palm}$ in comparison to soluble rPrP, indicating a partial protection of the predominantly α-helical, cellular form of $rPrP^{Palm}$. An important step toward the elucidation of prion conversion and prion turnover was achieved by a successful transfer of semisynthetic $rPrP^{Palm}$ into the plasma membrane of live cells.

EXPERIMENTAL PROCEDURES

All chemicals used were obtained from Sigma-Aldrich and Novabiochem in the highest purity available if not otherwise stated.

Peptide Synthesis

Solid-phase peptide synthesis was performed on a custom-modified 433A peptide synthesizer from Applied Biosystems, by using Boc

chemistry, in situ neutralization, and HBTU activation protocols [45] or by manually using Fmoc chemistry [46]. Cleavage of ivDde-protecting groups was carried out with 3% hydrazine in dimethylformamide (DMF), and palmitoylation was done with 20 eq. palmitoylchloride, 20 eq. HOBT, and 22 eq. triethylamine in dichloromethane (DCM)/DMF (3:1) for 4 hr. Removal of Mmt was achieved by treatment with acetic acid, trifluorethanol, and DCM (1:2:7), after neutralizing the resin with 10% DIEA in DMF. Cy5 coupling was performed by the addition of Cy5-NHS for 24 hr. Peptides synthesized by Boc chemistry were deprotected and simultaneously cleaved from the resin by using anhydrous hydrogen fluoride, whereas those synthesized by Fmoc chemistry were cleaved by 2.5% H_2O and 5% TIS in TFA. Crude products were subsequently precipitated with diethyl ether, dissolved in 50% aqueous acetonitrile (0.1% TFA), and lyophilized. Peptides were purified by RP-HPLC on C4 columns from Vydac by using linear gradients of buffer B (acetonitrile with 0.08% trifluoroacetic acid) in buffer A (water with 0.1% trifluoroacetic acid).

HPLC and Mass Spectrometry

HPLC analysis of peptides was performed on an analytical RP-C4 column (Vydac) (Hesperia, CA) at a flow rate of 1 ml/min over 30 min with a gradient from 5% to 80% (v/v) buffer B in buffer A. Peptide and protein masses were determined by electrospray ionization mass spectrometry on an LCQ Advantage Max (Finnigan) operating in positive ion mode. The molecular masses were deconvoluted from the charged ion spectra.

Native Chemical Ligation

Native chemical ligations of synthetic peptides were carried out in 6 M GdnHCl, 300 mM NaP_i, 1% (v/v) thiophenol (optional addition of 17 mg/ml dodecylphosphocholine [DPC]) at pH 7.4–7.7 by using concentrations of 5–6 mM of C- and N-terminal peptides [30]. Native chemical ligation reactions of rPrP thioester with peptides **1**–**5** were carried out in 8 M urea, 300 mM NaP_i, 17 mg/ml DPC, and 1% (v/v) thiophenol at pH 7.8 and concentrations of 1 mM rPrP thioester and 1.5–2 equivalents of peptides **1**–**5**.

Reactions were quenched by the addition of 3 volume equivalents of ligation buffer and 20% (v/v) β-mercaptoethanol. The ligation mixtures were purified by RP-HPLC on a C4 column from Vydac with linear gradients.

Expression and Purification of Recombinant rPrP

Recombinant murine rPrP(90–232) was cloned into a modified pTXB3 vector (New England Biolabs) containing the GyrA mini-intein and a chitin-binding domain (CBD) with an additional His tag between them. Expression was carried out in *E. coli* BL21(DE3), and cells were harvested and lysed as described below. Solubilization of inclusion bodies was achieved in 8 M urea, followed by affinity purification with Ni-NTA (QIAGEN). After dialysis against a buffer containing 4 M urea and 50 mM Tris-HCl (pH 8.0), a 50 mM NaCl addition of 250 mM MESNA was used to form the rPrP thioester. The rPrP thioester was purified via a C4-RP-HPLC column (Vydac) by applying a gradient of 35% buffer B in buffer A to 70% buffer B in buffer A over 60 min. Typical yields were 20 mg of rPrP-GyrA fusion construct from 1 l of *E. coli* culture that resulted in 2 mg of HPLC-purified rPrP thioester.

Recombinant murine rPrP(90–232) was cloned into the pTXB3 (New England Biolabs) vector and expressed in *E. coli* BL21(DE3)RIL as a fusion protein with the $DnaE^N$ split intein from *Synechocystis* and an additional His tag. Protein expression was induced with IPTG and gave ~20 mg rPrP-$DnaE^N$ fusion protein per 1 l *E. coli* culture. The cells were harvested by centrifugation and lysed in a M110S Microfluidizer (Microfluids Corporation, Newton). rPrP-$DnaE^N$-His was deposited in inclusion bodies and had to be dissolved in 8 M GdnHCl prior to Ni-NTA (QIAGEN) purification.

Folding of rPrP-$DnaE^N$-His

The denatured protein was diluted 1:10 to a final concentration of 0.1 mg/ml into a buffer containing 0.6 M L-arginine, 50 mM Tris-HCl (pH 8.6), and 5 mM GSH/0.5 mM GSSG. The solution was incubated for 12 hr at 4°C. L-arginine and the redox agents were removed by dialysis against 50 mM Tris-HCl buffer (pH 7.5). Folding yields were ~50%, leading to 10 mg rPrP-$DnaE^N$ for *trans*-splicing reactions from 1 l *E. coli* culture. The protein solution was concentrated to 10 μM rPrP-$DnaE^N$-His.

Trans-Splicing of rPrP-$DnaE^N$-His

Protein *trans*-splicing of rPrP-$DnaE^N$ and $DnaE^C$-guanidine hydrochloride (GPI) anchor mimics was carried out at equimolar concentrations of 5 μM in 50 mM Tris-HCl (pH 8) (*trans*-splicing buffer) in the presence of 50 mM MESNA and optional addition of octylglycoside (OG) or 1,2-dioleoyl-*sn*-glycero-3-phosphocholine (DOPC) liposomes. Reactions were stopped by the addition of SDS sample buffer for SDS-PAGE analysis or by transfer into 6 M GdnHCl buffer (see below). Purification was achieved by affinity chromatography with Ni-NTA fast-flow Sepharose (QIAGEN) in 6 M GdnHCl buffer to remove unreacted rPrP-$DnaE^N$ and $DnaE^N$. Subsequent size-exclusion chromatography (Superdex 75, Pharmacia) allowed for separation of $rPrP^{Palm}$.

Folding of $rPrP^{Palm}$ Variants

The proteins were incubated in 6 M GdnHCl, 50 mM Tris-HCl (pH 7.5) containing 5 mM GSH and 0.5 mM GSSG for 1 hr. Gel filtration was used to exchange the GdnHCl-containing buffer against 20 mM NaOAc (pH 5.5) (folding buffer) containing 20 mM OG. The protein solution was concentrated to 10 μM. Combined yields of the *trans*-splicing reaction between rPrP-$DnaE^N$ and peptides **1**–**5** linked to $DnaE^C$ as well as the folding of the resulting splicing products $rPrP^{Palm}$ were typically ~20%, leading to 2 mg $rPrP^{Palm}$ from 1 l *E. coli* culture.

Preparation of Liposomes

DOPC lipids were solved in DCM, and a thin lipid film was formed by evaporation of the solvent under rotation in a helium stream. The lipid film was hydrated in either *trans*-splicing or folding buffer for 1 hr. Formation of small unilamellar vesicles (SUVs) was achieved by sonication and subsequent centrifugation at 100,000 × g for 30 min at 22°C.

Dynamic Light Scattering

The size of SUVs was checked by dynamic light scattering on a DynaPro system (Wyatt Technology).

Reconstitution of Lipidated Samples

Lipidated refolded proteins were diluted (10-fold) into a 10 mg/ml SUV solution. The samples were dialysed overnight against biobeads (Biorad) containing phosphate-buffered saline (PBS) buffer.

CD Spectroscopy

Far-UV CD spectra were recorded on a Jasco J-715 spectropolarimeter. Protein concentrations were 0.2 mg/ml in 20 mM NaOAc at pH 5.5. All spectra were recorded in a 0.1 cm cuvette between 200 and 250 nm.

Fibril Formation

α-helical rPrP and $rPrP^{Palm}$ were dialysed against 3 M urea, 1 M GdnHCl, 150 mM NaCl, and 20 mM NaPi (pH 6.8) as reported previously [47]. Samples were incubated at room temperature for 1–4 days. Aggregation was followed by either proteinase K resistance or thioflavin T fluorescence.

Proteolysis of rPrP and $rPrP^{Palm}$

Proteinase K (Sigma) was used to digest rPrP variants with a substrate to enzyme ratio of 50:1 at 37°C for 1 hr in 100 mM Tris-HCl (pH 7.5). Digestion was stopped by the addition of 2 mM PMSF. Treated samples were analyzed by SDS/PAGE.

ThT Assay

Aliquots withdrawn during incubation of rPrP and $rPrP^{Palm}$ in aggregation buffer were diluted into 5 mM sodium acetate buffer (pH 5.5) to

a final concentration of 0.3 μM rPrP and $rPrP^{Palm}$. ThT (Sigma) was added to a final concentration of 10 μM. The emission spectra (from 460 nm to 520 nm) were recorded with excitation at 445 nm on a LS 55 Spectrometer (PerkinElmer). The fluorescence intensities at emission maximum (488 nm) were determined and plotted against time.

Cell Lysis and Western Blot

As described earlier [48], cells were washed twice with cold saline buffer (PBS), scraped off the plate, pelleted by centrifugation, and lysed in cold buffer C (0.5% Triton X-100, 0.5% sodium deoxycholate [DOC] in PBS). After centrifugation, the detergent-soluble and -insoluble fractions were analyzed by western blot. SDS-PAGE and western blot were described previously [39].

Transfection

Mouse N2a and HEK293T cells were cultivated as described [18]. Cells were transfected by liposome-mediated transfer by using Pro-Ject protein transfection reagent according to the manufacturer's instruction (Pierce).

Assay for Uptake of $rPrP^{Palm}$

To examine the amount of untransfected recombinant PrP, the medium was collected and PrP was precipitated with trichloroacetic acid (TCA) and analyzed by western blot with the monoclonal antibody 3F4. The cells were washed three times with cold PBS, scraped off the plate, pelleted by centrifugation, and lysed in cold buffer (0.5% Triton X-100 and 0.5% sodium DOC in PBS). The lysate was centrifuged at 15,000 × g for 20 min at 4°C. After boiling the supernatant and the pellet in Lämmli sample buffer, the samples were analyzed by immunoblotting.

Indirect Immunofluorescence

As described earlier [49], cells were grown on glass coverslips, fixed with 3% paraformaldehyde for 20 min, and permeabilized with 0.2% Triton X-100 for 10 min at room temperature. The primary antibody was incubated for 45 min at 37°C in PBS containing 1% BSA. After extensive washing with cold PBS, an incubation with Cy3-conjugated anti-mouse antibody (Dianova) (dilution 1:200) followed at 37°C for 30 min. The washed glass coverslips were mounted onto glass slides and examined by fluorescence microcopy (Axiovert 200 M, Zeiss) by using the AxioVision 3.0 software.

The plasmid encoding PrPC used as control in immunofluorescence experiments was described previously [18]. Cultivated N2a and HEK293T cells were transfected with a total of 1 μg DNA by using a liposome-mediated method with LipofectAmine Plus reagent (Invitrogen) according to the manufacturer's instructions.

Flotation Assay

Lysis of N2a cells was carried out in 200 μl MBS buffer (25 mM MES, 150 mM NaCl [pH 6.5]) with 1% Triton X-100 at 4°C. After low-spin centrifugation (5 min, 500 × g), 200 μl MBS containing 80% sucrose was added to the supernatant. The resulting 400 μl was covered with 3 ml 30% sucrose and 1 ml 5% sucrose in MBS buffer.

The resulting step gradient was centrifuged overnight (40,000 rpm, MLS 50, 4°C) and analyzed in 500 μl fractions by western blot as described above.

Supplemental Data

Supplemental Data include analytical information on the GPI anchor-mimicking peptides and are available at http://www.chembiol.com/cgi/content/full/14/9/994/DC1/.

ACKNOWLEDGMENTS

The authors would like to thank Sascha Gentz for technical assistance and Roger Goody for continuous support. This work was funded by the Max-Planck Society and the Deutsche Forschungsgemeinschaft (SFB 596).

Received: February 15, 2007
Revised: July 16, 2007
Accepted: August 1, 2007
Published: September 21, 2007

REFERENCES

1. Weissmann, C., Fischer, M., Raeber, A., Bueler, H., Sailer, A., Shmerling, D., Rulicke, T., Brandner, S., and Aguzzi, A. (1996). The role of PrP in pathogenesis of experimental scrapie. Cold Spring Harb. Symp. Quant. Biol. *61*, 511–522.
2. Prusiner, S.B., Scott, M.R., DeArmond, S.J., and Cohen, F.E. (1998). Prion protein biology. Cell *93*, 337–348.
3. Collinge, J. (2001). Prion diseases of humans and animals: their causes and molecular basis. Annu. Rev. Neurosci. *24*, 519–550.
4. Chesebro, B. (2003). Introduction to the transmissible spongiform encephalopathies or prion diseases. Br. Med. Bull. *66*, 1–20.
5. Aguzzi, A., and Polymenidou, M. (2004). Mammalian prion biology: one century of evolving concepts. Cell *116*, 313–327.
6. Meyer, R.K., Mckinley, M.P., Bowman, K.A., Braunfeld, M.B., Barry, R.A., and Prusiner, S.B. (1986). Separation and properties of cellular and scrapie prion proteins. Proc. Natl. Acad. Sci. USA *83*, 2310–2314.
7. Pan, K.M., Baldwin, M., Nguyen, J., Gasset, M., Serban, A., Groth, D., Mehlhorn, I., Huang, Z.W., Fletterick, R.J., Cohen, F.E., and Prusiner, S.B. (1993). Conversion of α-helices into β-sheets features in the formation of the scrapie prion proteins. Proc. Natl. Acad. Sci. USA *90*, 10962–10966.
8. Safar, J., Roller, P.P., Gajdusek, D.C., and Gibbs, C.J. (1993). Thermal stability and conformational transitions of scrapie amyloid (prion) protein correlate with infectivity. Protein Sci. *2*, 2206–2216.
9. Hope, J., Morton, L.J.D., Farquhar, C.F., Multhaup, G., Beyreuther, K., and Kimberlin, R.H. (1986). The major polypeptide of scrapie-associated fibrils (SAF) has the same size, charge distribution and N-terminal protein sequence as predicted for the normal brain protein (PrP). EMBO J. *5*, 2591–2597.
10. Turk, E., Teplow, D.B., Hood, L.E., and Prusiner, S.B. (1988). Purification and properties of the cellular and scrapie hamster prion proteins. Eur. J. Biochem. *176*, 21–30.
11. Stahl, N., Borchelt, D.R., Hsiao, K., and Prusiner, S.B. (1987). Scrapie prion protein contains a phosphatidylinositol glycolipid. Cell *51*, 229–240.
12. Stahl, N., Baldwin, M.A., Hecker, R., Pan, K.M., Burlingame, A.L., and Prusiner, S.B. (1992). Glycosylinositol phospholipid anchors of the scrapie and cellular prion proteins contain sialic acid. Biochemistry *31*, 5043–5053.
13. Gorodinsky, A., and Harris, D.A. (1995). Glycolipid-anchored proteins in neuroblastoma cells form detergent-resistant complexes without caveolin. J. Cell Biol. *129*, 619–627.
14. Taylor, D.R., and Hooper, N.M. (2006). The prion protein and lipid rafts. Mol. Membr. Biol. *23*, 89–99.
15. Critchley, P., Kazlauskaite, J., Eason, R., and Pinheiro, T.J.T. (2004). Binding of prion proteins to lipid membranes. Biochem. Biophys. Res. Commun. *313*, 559–567.
16. Taraboulos, A., Scott, M., Semenov, A., Avraham, D., Laszlo, L., and Prusiner, S.B. (1995). Cholesterol depletion and modification of COOH-terminal targeting sequence of the prion protein inhibit formation of the scrapie isoform. J. Cell Biol. *129*, 121–132.
17. Kaneko, K., Vey, M., Scott, M., Pilkuhn, S., Cohen, F.E., and Prusiner, S.B. (1997). COOH-terminal sequence of the cellular prion protein directs subcellular trafficking and controls conversion into the scrapie isoform. Proc. Natl. Acad. Sci. USA *94*, 2333–2338.

18. Winklhofer, K.F., Heske, J., Heller, U., Reintjes, A., Muranyi, W., Moarefi, I., and Tatzelt, J. (2003). Determinants of the in vivo folding of the prion protein. A bipartite function of helix 1 in folding and aggregation. J. Biol. Chem. *278*, 14961–14970.

19. Morillas, M., Swietnicki, W., Gambetti, P., and Surewicz, W.K. (1999). Membrane environment alters the conformational structure of the recombinant human prion protein. J. Biol. Chem. *274*, 36859–36865.

20. Baron, G.S., Wehrly, K., Dorward, D.W., Chesebro, B., and Caughey, B. (2002). Conversion of raft associated prion protein to the protease-resistant state requires insertion of PrP-res (PrP(Sc)) into contiguous membranes. EMBO J. *21*, 1031–1040.

21. Baron, G.S., and Caughey, B. (2003). Effect of glycosylphosphatidylinositol anchor-dependent and -independent prion protein association with model raft membranes on conversion to the protease-resistant isoform. J. Biol. Chem. *278*, 14883–14892.

22. Eberl, H., Tittmann, P., and Glockshuber, R. (2004). Characterization of recombinant, membrane-attached full-length prion protein. J. Biol. Chem. *279*, 25058–25065.

23. Hicks, M.R., Gill, A.C., Bath, I.K., Rullay, A.K., Sylvester, I.D., Crout, D.H., and Pinheiro, T.J.T. (2006). Synthesis and structural characterization of a mimetic membrane-anchored prion protein. FEBS J. *273*, 1285–1299.

24. Weissmann, C. (1995). Molecular biology of prion diseases. AIDS Res. Hum. Retroviruses *11*, S71–S72.

25. Prusiner, S.B. (1998). Prions. Proc. Natl. Acad. Sci. USA *95*, 13363–13383.

26. Aguzzi, A., and Heppner, F.L. (2000). Pathogenesis of prion diseases: a progress report. Cell Death Differ. *7*, 889–902.

27. Priola, S.A., and Vorberg, I. (2004). Identification of possible animal origins of prion disease in human beings. Lancet *363*, 2013–2014.

28. Breydo, L., Sun, Y., Makarava, N., Lee, C.I., Novitskaia, V., Bocharova, O., Kao, J.P.Y., and Baskakov, I.V. (2007). Nonpolar substitution at the C-terminus of the prion protein, a mimic of the glycosylphosphatidylinositol anchor, partially impairs amyloid fibril formation. Biochemistry *46*, 852–861.

29. Muir, T.W. (2003). Semisynthesis of proteins by expressed protein ligation. Annu. Rev. Biochem. *72*, 249–289.

30. Dawson, P.E., Muir, T.W., Clark-Lewis, I., and Kent, S.B.H. (1994). Synthesis of proteins by native chemical ligation. Science *266*, 776–779.

31. Martin, D.D., Xu, M.Q., and Evans, T.C., Jr. (2001). Characterization of a naturally occurring trans-splicing intein from *Synechocystis* sp. PCC6803. Biochemistry *40*, 1393–1402.

32. Giriat, I., and Muir, T.W. (2003). Protein semi-synthesis in living cells. J. Am. Chem. Soc. *125*, 7180–7181.

33. Zacharias, D.A., Violin, J.D., Newton, A.C., and Tsien, R.Y. (2002). Partitioning of lipid-modified monomeric GFPs into membrane microdomains of live cells. Science *296*, 913–916.

34. Rose, K., and Vizzavona, J. (1999). Stepwise solid-phase synthesis of polyamides as linkers. J. Am. Chem. Soc. *121*, 7034–7038.

35. Becker, C.F., Oblatt-Montal, M., Kochendoerfer, G.G., and Montal, M. (2004). Chemical synthesis and single channel properties of tetrameric and pentameric TASPs (template-assembled synthetic proteins) derived from the transmembrane domain of HIV virus protein u (Vpu). J. Biol. Chem. *279*, 17483–17489.

36. Sydor, J.R., Mariano, M., Sideris, S., and Nock, S. (2002). Establishment of intein-mediated protein ligation under denaturing conditions: C-terminal labeling of a single-chain antibody for biochip screening. Bioconjug. Chem. *13*, 707–712.

37. Schelhaas, M., Nagele, E., Kuder, N., Bader, B., Kuhlmann, J., Wittinghofer, A., and Waldmann, H. (1999). Chemoenzymatic synthesis of biotinylated Ras peptides and their use in membrane binding studies of lipidated model proteins by surface plasmon resonance. Chem. Eur. J. *5*, 1239–1252.

38. Riek, R., Hornemann, S., Wider, G., Billeter, M., Glockshuber, R., and Wüthrich, K. (1996). NMR structure of the mouse prion protein domain PrP(121-321). Nature *382*, 180–182.

39. Winklhofer, K.F., and Tatzelt, J. (2000). Cationic lipopolyamines induce degradation of PrPSc in scrapie-infected mouse neuroblastoma cells. Biol. Chem. *381*, 463–469.

40. Kascsak, R.J., Rubenstein, R., Merz, P.A., Tonna-DeMasi, M., Fersko, R., Carp, R.I., Wisniewski, H.M., and Diringer, H. (1987). Mouse polyclonal and monoclonal antibody to scrapie-associated fibril proteins. J. Virol. *61*, 3688–3693.

41. Brown, D.A., and Rose, J.K. (1992). Sorting of GPI-anchored proteins to glycolipid-enriched membrane subdomains during transport to the apical cell surface. Cell *68*, 533–544.

42. Vey, M., Pilkuhn, S., Wille, H., Nixon, R., DeArmond, S.J., Smart, E.J., Anderson, R.G., Taraboulos, A., and Prusiner, S.B. (1996). Subcellular colocalization of the cellular and scrapie prion proteins in caveolae-like membranous domains. Proc. Natl. Acad. Sci USA *93*, 14945–14949.

43. Kaneko, K., Wille, H., Mehlhorn, I., Zhang, H., Ball, H., Cohen, F.E., Baldwin, M.A., and Prusiner, S.B. (1997). Molecular properties of complexes formed between the prion protein and synthetic peptides. J. Mol. Biol. *270*, 574–586.

44. Sanghera, N., and Pinheiro, T.J. (2002). Binding of prion protein to lipid membranes and implications for prion conversion. J. Mol. Biol. *315*, 1241–1256.

45. Schnölzer, M., Alewood, P., Jones, A., Alewood, D., and Kent, S.B.H. (1992). In situ neutralization in Boc-chemistry solid phase peptide synthesis. Rapid, high yield assembly of difficult sequences. Int. J. Pept. Protein Res. *40*, 180–193.

46. Atherton, B., and Sheppard, R.C. (1989). Solid Phase Peptide Synthesis: A Practical Approach (Oxford: IRL Press at Oxford University Press).

47. Bocharova, O.V., Breydo, L., Parfenov, A.S., Salnikov, V.V., and Baskakov, I.V. (2005). In vitro conversion of full-length mammalian prion protein produces amyloid form with physical properties of PrP(Sc). J. Mol. Biol. *346*, 645–659.

48. Tatzelt, J., Prusiner, S.B., and Welch, W.J. (1996). Chemical chaperones interfere with the formation of scrapie prion protein. EMBO J. *15*, 6363–6373.

49. Rambold, A.S., Miesbauer, M., Rapaport, D., Bartke, T., Baier, M., Winklhofer, K.F., and Tatzelt, J. (2006). Association of Bcl-2 with misfolded prion protein is linked to the toxic potential of cytosolic PrP. Mol. Biol. Cell *17*, 3356–3368.

 ©2007 Elsevier Ltd All rights reserved